Wang, J. J., Wang, Y. Q., Cao, F. F., Guo, Y. G. & Wan, L. J. Synthesis of monodispersed wurtzite structure CuInSe2 nanocrystals and their application in high-performance organic-n...

ARTICLE *in* JOURNAL OF THE AMERICAN CHEMICAL SOCIETY · SEPTEMBER 2010

Impact Factor: 12.11 · DOI: 10.1021/ja1057955 · Source: PubMed

J|A|C|S COMMUNICATIONS

Published on Web 08/16/2010

Synthesis of Monodispersed Wurtzite Structure $CuInSe_2$ Nanocrystals and Their Application in High-Performance Organic−Inorganic Hybrid Photodetectors

Jian-Jun Wang, Yong-Qing Wang, Fei-Fei Cao, Yu-Guo Guo,* and Li-Jun Wan*

Key Laboratory of Molecular Nanostructure and Nanotechnology and Beijing National Laboratory for Molecular Sciences, Institute of Chemistry, Chinese Academy of Sciences, Beijing 100190, China

Received June 30, 2010; E-mail: ygguo@iccas.ac.cn; wanlijun@iccas.ac.cn

Abstract: A new facile solution method for the synthesis of high-quality $CuInSe_2$ nanocrystals with monodispersed size and uniform hexagonal shape was developed. A high-performance hybrid photodetector based on a hybrid film of $CuInSe_2$ nanocrystals and poly(3-hexylthiophene) was constructed. The device showed distinct "ON" and "OFF" states with a ratio of >100 in photocurrents responding to outside illumination. The high sensitivity and stability of the hybrid device revealed a broad prospect for use of the hybrid material in light detection and signal magnification for the development of large-area, low-cost, lightweight, and foldable products.

Photoelectric devices based on organic molecules and polymers have attracted considerable attention recently because of their unique properties.[1−7] First of all, the fast development of solution-based synthetic methods for organic materials has enabled their large-scale production at low cost. In addition, organic chemistry offers ample techniques for tuning their functions by modifying the structures of the molecules or the monomers of the polymers.[1,2,4,8] In particular, the exceptional mechanical flexibility of organic materials makes them perfect candidates for use in lightweight and foldable devices[1,2,4,6,7] However, despite the rapid advancement in organic photoelectrics, a well-recognized problem regarding their practical application lies in the extremely low carrier mobility and the peculiarly limited light absorption range, which has greatly deteriorated the performance of organic material-based photoelectric devices.

In comparison with their organic counterparts, inorganic nanocrystal-based photoelectric devices possess high device efficiencies, benefiting from their superior intrinsic carrier mobilities and broadband absorption.[9−15] Meanwhile the properties of semiconductor nanocrystals (NCs) have proved to be strongly size-dependent. Their emission and absorption can be easily engineered by their particle size as a result of the quantum confinement effect.[16,17] Therefore, various high-performance electronic and optical nanodevices have been demonstrated, including memories,[18] photodetectors,[12,14] field-effect transistors,[19] and solar cells.[9−11,20] On the other hand, because of the large surface-to-volume ratio, unpassivated orbitals at the NC surface and defects introduced by surface modifications detrimentally affect the photoelectric properties of NCs and reduce the efficiencies of the photoelectric devices.[17] Nonetheless, production of photoelectric devices with the advantages of both organic materials and inorganic nanomaterials is promising.

Hybrid organic−inorganic devices are a logical choice for combining the unique properties of NCs with the easy film-forming properties of organic polymers.[21−23] As the state of the art of organic chemistry has developed, many semiconducting polymers have been synthesized. This provides an avenue for constructing a new generation of hybrid organic−inorganic devices in which both components can be photovoltaically active.[7,22,23] Herein, we used the hybridization of inorganic $CuInSe_2$ (CISe) NCs and organic poly(3-hexylthiophene) (P3HT) as an example to demonstrate the construction of multiple photodetectors with high performance. P3HT is a classical π-electron-conjugated polymer with high electrical conductivity and strong absorption in the visible range.[24] CISe was selected not only because of its high absorption coefficient and appropriate band gap but also because of its high radiation stability.[9,10]

CISe colloidal NCs have attracted much attention because they are convenient for further processing via spin-casting, dip-coating, and printing, and more importantly, the corresponding devices exhibit high performance due to the quantum confinement effect.[22,25,26] In recent years, great progress has been made in the synthesis of colloidal CISe NCs.[9,10,25,27−34] Many synthetic routes, including solvothermal,[29] thermolysis,[25] microwave-assisted,[27] and hot-injection methods, have been reported.[9,10,32] The above methods need either special apparatus or unique precursors with tedious complicated synthesis procedures, and the synthesized NCs exhibit agglomeration or broad size distributions. The poor solubility in popular solvents of Se powder, which is often used either as the Se source or to stop the reaction between Cu and In sources, makes it especially difficult to prepare high-quality CISe NCs with a pure phase, let alone uniform CISe NCs with shape control. Consequently, it remains a big challenge to develop new routes for the synthesis of high-quality CISe NCs, especially solution-phase preparations. Here we report the synthesis of nearly monodispersed wurtzite structure CISe NCs with hexagonal shape and their high performance in a hybrid photodetector together with P3HT.

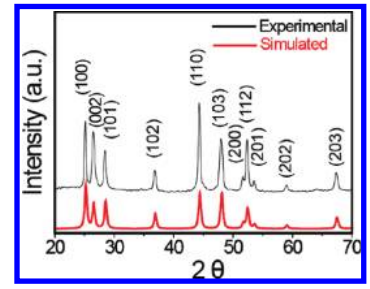

Figure 1. Experimental and simulated XRD patterns of CISe NCs with a wurtzite structure.

In our experiments, a Cu−oleate complex was first prepared from the reaction between $CuCl_2$ and sodium oleate, both of which are environmentally friendly and inexpensive. Diphenyl diselenide was selected as the selenide source to react with the Cu−oleate complex and $InCl_3$ [see the Supporting Information (SI)]. The synthesized NCs were capped with organic ligands, allowing them to disperse freely in organic solvents such as toluene and hexane. Moreover, the organic ligands initiate attractive forces with polymer chains, contributing to the formation of hybrid homogeneous films.[22]

10.1021/ja1057955

The structure of the as-synthesized NCs was characterized by X-ray diffraction (XRD), as shown in Figure 1. It was found that no existing patterns in the standard JCPDS database can match well with the one we acquired (Table S1 in the SI). Preliminary simulation revealed that such NCs hold a wurtzite phase (Figure S1 in the SI),[35] which is totally different from the well-characterized chalcopyrite type in the JCPDS database. As shown in Figure 1, the experimental pattern of the NCs matches well with the simulated one of wurtzite structure (a = 4.083 Å, c = 6.727 Å). It is also noteworthy that a strong (002) diffraction peak was observed for the NCs, indicating that the as-prepared wurtzite structure CISe (wz-CISe) NCs have an (002)-textured structure.

Figure 2a,b shows typical transmission electron microscopy (TEM) images of the CISe NCs. The large-area TEM images indicate that the as-synthesized NCs are nearly monodispersed with an average diameter of ~21.3 nm and that they easily self-assemble into 2D arrays because of their uniform hexagonal shape. Figure 2c shows a high-resolution TEM (HRTEM) image of an individual nanocrystal. The lattice fringes show that the NCs are well-crystallized, and the observed d spacings correspond to the (100) plane of CISe. The selected-area electron diffraction (SAED) pattern (Figure 2d) is also well-consistent with the simulated wurtzite structure of CISe. It should be pointed out that the SAED pattern contains not diffraction rings but instead diffraction arcs with hexagonal symmetry, indicating that the orientation of the atomic lattice of an individual nanocrystal self-assembled into a 2D array is not random but preferentially lies along the [001] direction.[15] In order to understand the formation process of the monodispersed products, synthesis experiments in the absence of $InCl_3$ were also performed. As can be seen from Figure S2, monodispersed CuSe nanocrystals were obtained. This result indicates that a possible mechanism for the monodispersion could be that diphenyl diselenide first reacts with the Cu−oleate complex to generate uniform seed crystals, which act as templates for the growth of monodispered CISe NCs after addition of $InCl_3$.

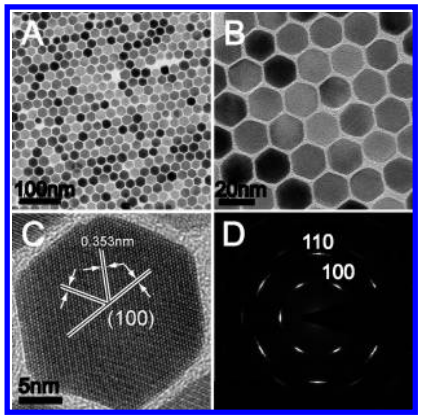

Figure 2. (a, b) TEM images of as-synthesized CISe NCs. (c) HRTEM image of a single CISe nanocrystal. (d) SAED pattern of as-synthesized CISe NCs.

To further identify the as-synthesized CISe NCs, the chemical composition was measured by energy-dispersive X-ray spectroscopy (EDS) (Figure S3), which confirmed that the NCs had a Cu/In/Se stoichiometric ratio of ~1:1:2. X-ray photoelectron spectroscopy (XPS) analysis showed that all three elements were in their expected oxidation states (Figure S4) and that the proportion of carbon was ~66.83 atom %. The large proportion of carbon indicates the presence of long alkyl groups (i.e., oleylamine) on the surface of the NCs in addition to the generally adsorbed gaseous molecules during XPS analysis. The binding energy of Cu $2p_{3/2}$ was 931.8 eV in the sample, which is consistent with that of monovalent copper. The result indicates that Cu^{2+} was reduced to Cu^{+} by oleylamine.[36] UV−vis absorption spectroscopy was utilized to estimate the band-gap energy of the wz-CISe NCs (Figure S5); the effective band gap was found to be 1.03 eV, which is in good agreement with the reported value of 1.04 eV for bulk CISe.[10,28]

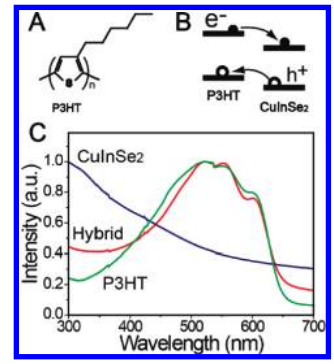

Figure 3. (a) Structure of P3HT. (b) Schematic energy-level diagram for CISe NCs and P3HT showing the charge transfer of electrons to the CISe NCs and holes to P3HT. (c) UV−vis spectra of the P3HT film (green), CISe NC film (blue), and P3HT:CISe hybrid film (~2:1 weight ratio) (red).

Figure 3c shows UV−vis spectra of a P3HT film (green), a CISe NC film (blue), and a P3HT:CISe NC hybrid film (~2:1 weight ratio) (red), which indicate that the inlay of CISe NCs into the P3HT film significantly broadens the absorption spectrum. A schematic illustration of a device based on the hybrid material is shown in Figure 4a. The gap width and electrode length were 35 and 125 μm, respectively. The device was fabricated by dropping 1 μL of hybrid solution onto precleaned electrodes and drying in air (see the SI). As shown in Figure S6, the hybrid film was highly smooth and homogeneous. The high absorption efficiency and the large interface between CISe NCs and P3HT are favorable for light absorption and exciton dissociation.

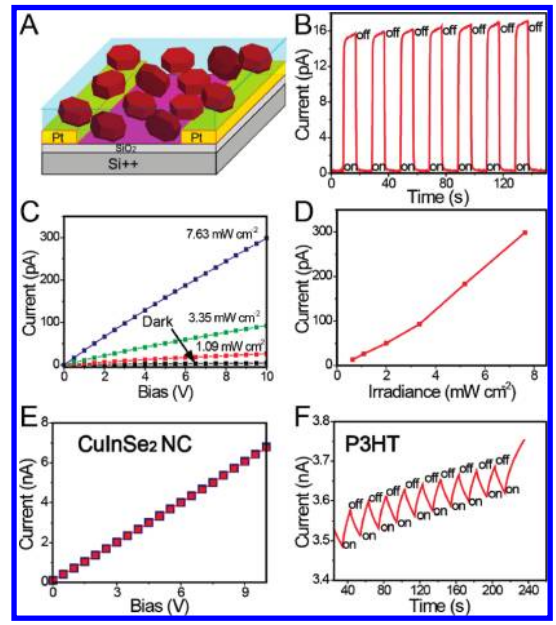

Figure 4. (a) Schematic illustration of the hybrid device. (b) On/off switching of the hybrid device at an incident light density of 7.63 mW cm^{-2} and a bias voltage of 0.4 V. (c) Dark current and photocurrents at different incident light densities. (d) Photocurrent measured as a function of incident light density at a bias voltage of 10 V. (e) Typical $I-V$ curves for an CISe NC film in the dark and at an incident light density of 7.63 mW cm^{-2}. (f) On/off switching of the device made from a pure P3HT film at an incident light density of 7.63 mW cm^{-2} and a bias voltage of 0.4 V.

The hybrid device exhibits excellent photoresponse characteristics, as shown in Figure 4b. An iodine−tungsten lamp was used as a white-light source. With the light irradiation on and off, the current in the devices showed two distinct states, a "low" current in the dark and a "high" current under illumination. The switching in these two states was very fast and reversible, allowing the device to act as a high-quality photosensitive switch. In the dark, the current was only 0.15 pA. However, at an incident light density of 7.63 mW cm^{-2} and a bias voltage of 0.4 V, the current could approach 17 pA, giving an on/off switching ratio of >100. The high photosensitivity of the hybrid devices was further confirmed by photocurrent measurements on the devices at different incident light densities. When the intensity of the incident light was changed, the photocurrent of the device remarkably changed accordingly (Figure 4c), which can be attributed to the change in the photon density of the incident light at different light densities. It is known that for hybrid organic−inorganic devices (e.g., MEH-PPV−CdSe NCs), light can be absorbed through the whole thickness of the device and that both types of charge carrier run within the device.[37] As shown in Figure 4d, the current of the present hybrid photodetector exhibited a strong dependence on light intensity, in agreement with the previous report on hybrid devices,[37] and demonstrated a power dependence of ∼1.34 (i.e., $I \sim P^{1.34}$), indicating superior photocurrent capability of the hybrid material. These results prove the promising potential of the hybrid device as a photoswitch and a highly photosensitive detector. It is worth noting that the applied bias voltage influenced the on/off ratio of the devices, which is a result of the applied bias voltage dependence of the exciton dissociation and the background current of the devices.

The interface of the P3HT:CISe hybrid film also plays a key role in the charge dissociation and transportation. Exciton dissociation is well-known to occur efficiently at the interface of two semiconductors mixed together in a blend film, such as a conjugated polymer and a fullerene derivative.[7,22,23] The photoexcited electrons can be accepted by the material with the higher electron affinity, while the hole can be caught by the material with the relatively lower ionization potential.[7,22,23] In our system, the CISe nanocrystal has a high electron affinity and could act as the photoelectron acceptor. Meanwhile, the P3HT is perfect for acting as a hole acceptor as well as an electron donor upon photoexcitation (Figure 3b). In the hybrid film, the CISe NCs are uniformly dispersed in the P3HT matrix, forming a three-dimensional interconnected network, which leads to a large interface area for charge separation. On the other hand, the different carriers have their own specific pathways to reach their corresponding electrodes; this effectively alleviates charge recombination, allowing the device to achieve a long-lived charge separation and high transportation.[22] In contrast, devices based on a film of pure CISe NCs showed no obvious photoresponse (Figure 4e) but had high resistivity due to the adsorbed insulating surfactants on their surface. The resistivity can be considerably reduced by exchanging these surfactants with short alkyl molecules (e.g., ethanethiol) or removing them (Figure S7).[37,38] In the case of the device made from pure P3HT, the photocurrent after illumination was relatively low and the on/off ratio was <2 (Figure 4f), consistent with previously reported results.[7] The feature of irreversible and low on/off switching demonstrates inefficient charge separation in the device without CISe NCs as the electron acceptors.[39] Notably, the OFF current in the hybrid device (∼0.15 pA) at a bias voltage of 0.4 V was lower than that of pure CISe (∼0.4 nA) or P3HT (∼0.35 nA) at the same bias, which could be attributed to the difficult charge transportation through the interfaces of P3HT and CISe without light illumination. The results indicate that both the sufficient light absorption of the hybrid film and the efficient charge dissociation at the interface of the hybrid material are critical for the construction of high-performance photodetectors. It should be noted that the hybrid photodectector also showed an outstanding stability. No obvious degradation was observed during extended hundreds of cycles. The high photoresponse performance together with its high stability makes the hybrid material a perfect candidate for light detection and signal magnification with prospects for applications in low-cost, lightweight, and foldable products.

In summary, a new facile solution method for the synthesis of high-quality $CuInSe_2$ NCs with monodispersed size, uniform hexagonal shape, and an optical band gap of 1.03 eV was developed. XRD, TEM, EDS, and XPS measurements confirmed that the NCs were pure wurtzite $CuInSe_2$. A high-performance hybrid photodetectors based on a P3HT:CISe hybrid film were constructed. The device showed distinct "ON" and "OFF" states with a photocurrent ratio of >100 in response to outside illumination. The high sensitivity and stability of the as-constructed device make the hybrid material a promising candidate for applications in light detection and signal magnification for the development of large-area, low-cost, lightweight, and foldable products.

Acknowledgment. This work was supported by the National Natural Science Foundation of China (Grants 20821003 and 50730005), the National Key Project on Basic Research (Grants 2006CB806100 and 2009CB930400), and the Chinese Academy of Sciences.

Supporting Information Available: Synthesis of the wurtzite CISe NCs; corresponding EDS, XPS, UV−vis absorption spectra; and SEM images of the wz-CISe and the P3HT:CISe hybrid film. This material is available free of charge via the Internet at http://pubs.acs.org.

References

(1) Baldo, M.; Deutsch, M.; Burrows, P.; Gossenberger, H.; Gerstenberg, M.; Ban, V.; Forrest, S. *Adv. Mater.* **1998**, *10*, 1505.
(2) Facchetti, A. *Mater. Today* **2007**, *10*, 28.
(3) Jiang, L.; Gao, J.; Wang, E.; Li, H.; Wang, Z.; Hu, W.; Jiang, L. *Adv. Mater.* **2008**, *20*, 2735.
(4) Li, R.; Hu, W.; Liu, Y.; Zhu, D. *Acc. Chem. Res.* **2010**, *43*, 529.
(5) Tang, Q.; Li, L.; Song, Y.; Liu, Y.; Li, H.; Xu, W.; Hu, W.; Zhu, D. *Adv. Mater.* **2007**, *19*, 2624.
(6) Tong, L.; Li, C.; Chen, F.; Bai, H.; Zhao, L.; Shi, G. *J. Phys. Chem. C* **2009**, *113*, 7411.
(7) Zhu, H.; Li, T.; Zhang, Y.; Dong, H.; Song, J.; Zhao, H.; Wei, Z.; Xu, W.; Hu, W.; Bo, Z. *Adv. Mater.* **2010**, *22*, 1645.
(8) Yan, Z.; Li, G. T.; Mu, L.; Tao, S. Y. *J. Mater. Chem.* **2006**, *16*, 1717.
(9) Brian, M.; Dunn, G.; Brian, A.; Korgel, A. *J. Am. Chem. Soc.* **2008**, *130*, 16770.
(10) Guo, Q.; Kim, S.; Kar, M.; Shafarman, W.; Birkmire, R.; Stach, E.; Agrawal, R.; Hillhouse, H. *Nano Lett.* **2008**, *8*, 2982.
(11) Gur, I.; Fromer, N. A.; Geier, M. L.; Alivisatos, A. P. *Science* **2005**, *310*, 462.
(12) Konstantatos, G.; Clifford, J.; Levina, L.; Sargent, E. *Nat. Photonics* **2007**, *1*, 531.
(13) Konstantatos, G.; Howard, I.; Fischer, A.; Hoogland, S.; Clifford, J.; Klem, E.; Levina, L.; Sargent, E. H. *Nature* **2006**, *442*, 180.
(14) Wang, J.-J.; Cao, F.-F.; Jiang, L.; Guo, Y.-G.; Hu, W.-P.; Wan, L.-J. *J. Am. Chem. Soc.* **2009**, *131*, 15602.
(15) Zhuang, Z.; Peng, Q.; Zhang, B.; Li, Y. *J. Am. Chem. Soc.* **2008**, *130*, 10482.
(16) Deng, Z.; Yan, H.; Liu, Y. *J. Am. Chem. Soc.* **2009**, *131*, 17744.
(17) Smith, A. M.; Nie, S. *Acc. Chem. Res.* **2009**, *43*, 190.
(18) Meister, S.; Peng, H.; McIlwrath, K.; Jarausch, K.; Zhang, X. F.; Cui, Y. *Nano Lett.* **2006**, *6*, 1514.
(19) Peng, H.; Xie, C.; Schoen, D. T.; Cui, Y. *Nano Lett.* **2008**, *8*, 1511.
(20) Wu, Y.; Wadia, C.; Ma, W.; Sadtler, B.; Alivisatos, A. P. *Nano Lett.* **2008**, *8*, 2551.
(21) Arici, E.; Hoppe, H.; Schaffler, F.; Meissner, D.; Malik, M. A.; Sariciftci, N. S. *Thin Solid Films* **2004**, *451−452*, 612.
(22) Günes, S.; Sariciftci, N. S. *Inorg. Chim. Acta* **2008**, *361*, 581.
(23) Huynh, W. U.; Dittmer, J. J.; Alivisatos, A. P. *Science* **2002**, *295*, 2425.
(24) Holdcroft, S. *Macromolecules* **1991**, *24*, 4834.
(25) Castro, S.; Bailey, S.; Raffaelle, R.; Banger, K.; Hepp, A. *Chem. Mater.* **2003**, *15*, 3142.

(26) Green, M.; Emery, K.; King, D.; Hishikawa, Y.; Warta, W. *Prog. Photovoltaics* **2007**, *15*, 35.
(27) Grisaru, H.; Palchik, O.; Gedanken, A.; Palchik, V.; Slifkin, M.; Weiss, A. *Inorg. Chem.* **2003**, *42*, 7148.
(28) Koo, B.; Patel, R.; Korgel, B. *J. Am. Chem. Soc.* **2009**, *131*, 3134.
(29) Li, B.; Xie, Y.; Huang, J.; Qian, Y. *Adv. Mater.* **1999**, *11*, 1456.
(30) Norako, M. E.; Brutchey, R. L. *Chem. Mater.* **2010**, *22*, 1613.
(31) Nose, K.; Omata, T.; Otsuka-Yao-Matsuo, S. *J. Phys. Chem. C* **2009**, *113*, 3455.
(32) Tang, J.; Hinds, S.; Kelley, S. O.; Sargent, E. H. *Chem. Mater.* **2008**, *20*, 6906.
(33) Xu, J.; Lee, C.-S.; Tang, Y.-B.; Chen, X.; Chen, Z.-H.; Zhang, W.-J.; Lee, S.-T.; Zhang, W.; Yang, Z. *ACS Nano* **2010**, *4*, 1845.
(34) Zhong, H.; Li, Y.; Ye, M.; Zhu, Z.; Zhou, Y.; Yang, C. *Nanotechnology* **2007**, *18*, 025602.
(35) Pan, D.; An, L.; Sun, Z.; Hou, W.; Yang, Y.; Yang, Z.; Lu, Y. *J. Am. Chem. Soc.* **2008**, *130*, 5620.
(36) Tang, J.; Konstantatos, G.; Hinds, S.; Myrskog, S.; Pattantyus-Abraham, A. G.; Clifford, J.; Sargent, E. H. *ACS Nano* **2009**, *3*, 331.
(37) Greenham, N. C.; Peng, X.; Alivisatos, A. P. *Phys. Rev. B* **1996**, *54*, 17628.
(38) Sun, B.; Marx, E.; Greenham, N. C. *Nano Lett.* **2003**, *3*, 961.
(39) Amos, F. F.; Morin, S. A.; Streifer, J. A.; Hamers, R. J.; Jin, S. *J. Am. Chem. Soc.* **2007**, *129*, 14296.

JA1057955